Environ. Sci. Technol. **2011,** *45,* 700–705

Determination of Dissolved Oxygen in the Cryosphere: A Comprehensive Laboratory and Field Evaluation of Fiber Optic Sensors

E. A. BAGSHAW,*,*,† J. L. WADHAM,† M. MOWLEM,‡ M. TRANTER,† J. EVENESS,†,|| A. G. FOUNTAIN,§ AND J. TELLING†

Bristol Glaciology Centre, University of Bristol, U.K., National Oceanography Centre, University of Southampton, U.K., and Departments of Geology and Geography, Portland State University, United States

Received September 6, 2010. Revised manuscript received November 17, 2010. Accepted November 22, 2010.

Recent advances in the Cryospheric Sciences have shown that icy environments are host to consortia of microbial communities, whose function and dynamics are often controlled by the concentrations of dissolved oxygen (DO) in solution. To date, only limited spot determinations of DO have been possible in these environments. They reveal the potential for rates of change that exceed realistic manual sampling rates, highlighting the need to explore methods for the continuous measurement of DO concentrations. We report the first comprehensive field and laboratory performance tests of fiber-optic sensors (PreSens, Regensburg, Germany) for measuring DO in icy ecosystems. A series of laboratory tests performed at low and standard temperatures (−5 to 20 °C) demonstrates high precision (0.3% at 50 μmol/kg and 1.3% at 300 μmol/kg), rapid response times (<20 s), and minimal drift (<0.4%). Survival of freeze thaw was problematic, unless the sensor film was mechanically fixed to the fiber and protected by a stainless steel sheath. Results of two field deployments of sensors to the Swiss Alps and Antarctica largely demonstrate a performance consistent with laboratory tests and superior to traditional methods.

Introduction

Dissolved oxygen (DO) is a key parameter in the estimation of biological activity in aquatic environments. The discovery that glaciers and ice sheets (including Antarctic subglacial lakes: Siegert et al. (*1*)) are host to significant populations of active microorganisms (*2*) has prompted a re-evaluation of the role of these environments in global biogeochemical cycles (*3*). Here, DO concentrations denote the balance between a range of processes, including biogeochemical reactions such as photosynthesis, respiration, and microbially mediated rock-water interactions such as sulfide oxidation (*4*). However, the use of traditional methods for the determination of DO in extreme icy climates is challenging. While traditional methods (Winkler titration and Clark Electrodes) have been employed for spot measurements (*5*−*7*), they do not offer an effective solution for continuous monitoring under many icy conditions, including deployment to Antarctic subglacial lakes.

The Winkler method involves the direct sampling of the water body. Oxygen in the water quantitatively oxidizes iodide to iodine, which is determined by titration with standardized thiosulfate solution (*8*). The procedure can be performed to a relatively high degree of accuracy (±0.05−0.1%) under optimum conditions (*9*). Field use requires relatively large sample volumes (~60 mL), and the methodology is sensitive to subzero air temperatures, since reagents may freeze. Frequent sampling for DO determination by this method in confined environments (e.g., cryoconite holes) may both deplete the available liquid water and perturb the DO concentration in the aquatic system under investigation. Measuring oxygen concentration with Clark-type electrodes (*10*) is less destructive, though these sensors consume some oxygen. Oxygen enters the sensor at a permeable membrane and is reduced at the cathode to produce an electrical current which is proportional to the DO concentration. The key disadvantages of this method are that the sensor must be fully immersed and requires constant stirring to replace oxygen depleted water at the sensor tip. Glacial aquatic environments often contain limited quantities of liquid water (*11*−*13*) so complete immersion of a large probe is not always possible, and a constant flow rate is rarely maintained. Periodic melting and freezing is also a problem for these electrodes. Commercially available microsensors (Unisense, Denmark) based on Clark electrodes have reduced the necessity for stirring, but their fine tipped glass construction makes them unsuitable for use in freeze thaw conditions.

Clearly, both traditional methods of determining DO in glacial aquatic environments have shortcomings, and there is a need to develop and validate new nondestructive methodologies which can obtain measurements with high temporal resolution, tolerate the extreme climate, and run for long periods without frequent recalibration. One of the optimum candidate technologies for this purpose is fiber optic sensors. Fiber optic microsensors were developed in the late 1980s and 1990s (*14, 15*) and are now commercially available (*16*). Typically, the exposed end of the fiber is coated with an immobilized indicator compound, which is sensitive to the measured parameter (*17*). A ruthenium complex is commonly used for the determination of DO. The luminescence of this indicator is quenched in the presence of oxygen (*15*). Luminescence quenching is frequently detected by analyzing intensity (*15*) or decay in the phase (*18*) or time domain (*19, 20*). Fiber optic sensors are advantageous for environmental monitoring because they a) consume no oxygen, b) are relatively portable, c) measure oxygen in both the gas and liquid phase, and d) require no stirring. They also have no cross-sensitivity with most common dissolved constituents in glacial meltwaters. They have been used effectively in aquatic and oceanographic studies (*15, 21, 22*), but there have been few applications to date in cryospheric settings (*23*). This study provides the first comprehensive laboratory and field evaluation of a commercially available fiber optic DO sensor for application within the Cryosphere.

Methodology

Laboratory tests were performed on PreSens Microx TX3 and Fibox 3 sensors (Regensburg, Germany). The ormosil-derived sensing film used by these sensors is based on a sol−gel

* Corresponding author phone: +44(0)1173314128; e-mail: Liz.Bagshaw@bristol.ac.uk.
† University of Bristol.
‡ University of Southampton.
|| Current address: ABB Sensors, Gloucestershire, U.K.
§ Portland State University.

10.1021/es102571j
Published on Web 12/01/2010

glass matrix and is characterized with a fiber optic setup illuminated by a blue LED (*24*). The Microx TX3 model was tested with two different microsensor probe types. Probe 1 was comprised of a tapered tip <50 μm exposed silica fiber. Probe 2 was a needle-type probe, where the 140 μm flat-broken tip silica optical fiber is contained in a syringe tip and only exposed during the measurement period. The Fibox 3 system was tested with two identical dipping probes (Probes 3 and 4), which consisted of a 2 mm polymer optical fiber contained in a stainless steel tube with a diameter of 4 mm. The exposed distal tip of the fiber was polished and coated with a planar oxygen sensitive foil which was mechanically fixed to the probe end.

The response of this luminescence lifetime indicator to variable DO concentration is governed by the Stern−Volmer equation (eq 1)

$$\frac{\tau o}{\tau} = 1 + K_{sv}[O_2] \quad (1)$$

where K_{sv} is the Stern−Volmer constant, $[O_2]$ is oxygen activity, governed by the partial pressure and solubility under Henry's Law (*25*), τo is the lifetime of fluorophore in the absence of oxygen, and τ is the lifetime of the fluorophore in the presence of oxygen (*26*).

The sensors use a phase modulation technique to evaluate the luminescent decay time of the indicator material. The phase angle shift between the exciting and emitted light signals is a function of the oxygen partial pressure. The relationship between the measured phase shift (Φ) and oxygen concentration $[O_2]$ is described by eq 2, where Φ_0 denotes the phase angle shift of oxygen-free water

$$[O_2] = \frac{\frac{\tan \Phi}{\tan \Phi_0} - 1}{K_{sv}} \quad (2)$$

Salinity and temperature corrections are applied (PreSens sensors have an additional external temperature probe), and DO concentration is calculated using a two point calibration, which generates the K_{sv} constant at varying temperatures. Phase shift, temperature, and the predicted oxygen saturation or concentration (% air saturation or mg/L) were logged on the PC by the Microx and Fibox Oxyview software.

Performance Tests. Performance tests were undertaken at temperatures between −5 and +20 °C in cold rooms and a cooled incubator (LMS Ltd.) at the University of Bristol's Low Temperature Experimental Facility (LOWTEX). The sensors were connected to a PC via a serial port and run with Microx (Probes 1 and 2) and Fibox (Probes 3 and 4) Oxyview software (PreSens Gmbh).

Response Time. Sensor response time (*t90*, the time in seconds when 90% of the change in phase angle has occurred in response to a step change in oxygen concentration in either the gas or aqueous phase) was evaluated in air and solution at 5 and 20 °C. Probes 2, 3, and 4 were tested in water-saturated air (assumed to be 100% air-saturated with oxygen) and a saturated solution of $NaSO_3$ (deoxygenated). Probe 1 was not tested.

Drift. The oxygen-sensitive luminescent coating of the sensor tip may degrade over time as a result of photobleaching, the extent of which depends on the intensity of the excitation light source and the measurement frequency (*15, 16, 22*). The percentage drift in measurement was assessed in a deoxygenated solution in the laboratory over 65 h with a measurement frequency of 1−2 s for Probes 1 and 2. Drift during field tests drift was also estimated for Probes 3 and 4 via repeated measurement of calibration solutions before, during, and after the field deployment (see below). Percentage drift was calculated from the change in the output phase shift of the solutions over time.

Freeze Thaw Cycles. The performance of the sensors during freeze−thaw cycling was assessed as follows. Probes 2 and 3 were suspended in a 50 mL centrifuge tube of deionized water, which was subjected to temperature variations between 10 and −8 °C. The temperature cycling consisted of 4 h at 10 °C, an 8 h transition between 10 and −8 °C, 8 h at −8 °C, and finally a 4 h transition to 10 °C. The probes were calibrated prior to the experiment, and the calibration was checked by monitoring the phase angle after the second and fifth freeze−thaw cycles. Both tips were photographed under a microscope before and after the freeze thaw tests.

Temperature Dependence and Accuracy. A DO test rig, as described in Sosna et al. (*27*), was programmed to provide an incremental increase in oxygen from 0 to 100% air-saturation in solution in twenty discrete steps. Oxygen saturated and oxygen free solutions were progressively mixed in a closed system at atmospheric pressure. The quantity of oxygen saturated solution sequentially added was controlled by a valve and solenoid pump and stirred for 2 min after each addition. The temperature was controlled by a thermostatic unit and could be varied from −5 to 20 °C. Readings were allowed to stabilize, and the phase shift and measured DO were logged for one minute by the PreSens software. The DO computed from the phase shift by the Presens software was compared with the absolute oxygen concentration determined by the calibration rig at five different temperatures (−5, 1, 5, 11, and 20 °C), with the raw phase shift, and the DO derived from Winkler titrations at 0, 50, and 100% O_2 air saturation at 20 °C.

Performance Comparison with Other Methods. The relative accuracy of the sensors in comparison with more traditional methods for determining DO was assessed as follows. Probes 1 and 2 were compared with Winkler titration at 0, 50, and 100% saturation, as determined by the test rig described above, at 20 °C. Probes 3 and 4 were compared to both Winkler titration and a Clark-type electrode across a range of oxygen concentrations at 5 and 20 °C. The Clark-type electrode was a YSI 550A (YSI Hydrodata, Yellow Springs, Ohio), calibrated using single-point air saturation. For these latter tests the degree of oxygen air saturation was controlled by progressive addition of air-saturated deionized water to N_2 saturated deionized water in a water bath.

Winkler titration was performed as in a field laboratory, and so without a magnetic stirring bar, digital end point determination, or argon gas atmosphere (*28*). Full details of this procedure can be found in the Supporting Information.

The evaluation of Probe 1 was discontinued after these performance and intercomparison tests. The probe displayed decreasing sensitivity to the higher oxygen concentrations found in many glacial aquatic environments. This, when coupled with the extreme fragility of the unprotected fiber, meant that the probe design was ultimately unsuited to field operation. Further testing of the Microx system continued with Probe 2, which had a more robust fiber and was protected by a needle-sheath when not in use.

Field Deployment. Probes 3 and 4 were field-tested by deployment to meltwater streams in the Swiss Alps (20−25th April 2009) and in small ice-enclosed water bodies on a glacier surface in the Dry Valleys of Antarctica (14−26th December 2008). The sensors were powered by 12 V 7Ah solar charged lead acid batteries and data were logged using a Campbell Scientific CR10X datalogger (Supporting Information: Figure I). The sensors were connected to the datalogger via coaxial BNC cables from the sensor analogue outputs. Frequency of illumination of the LED, and hence measurement frequency, was controlled by a pulsed trigger port output from the datalogger. Water temperature, air temperature, electrical conductivity, DO, and battery voltage were measured every

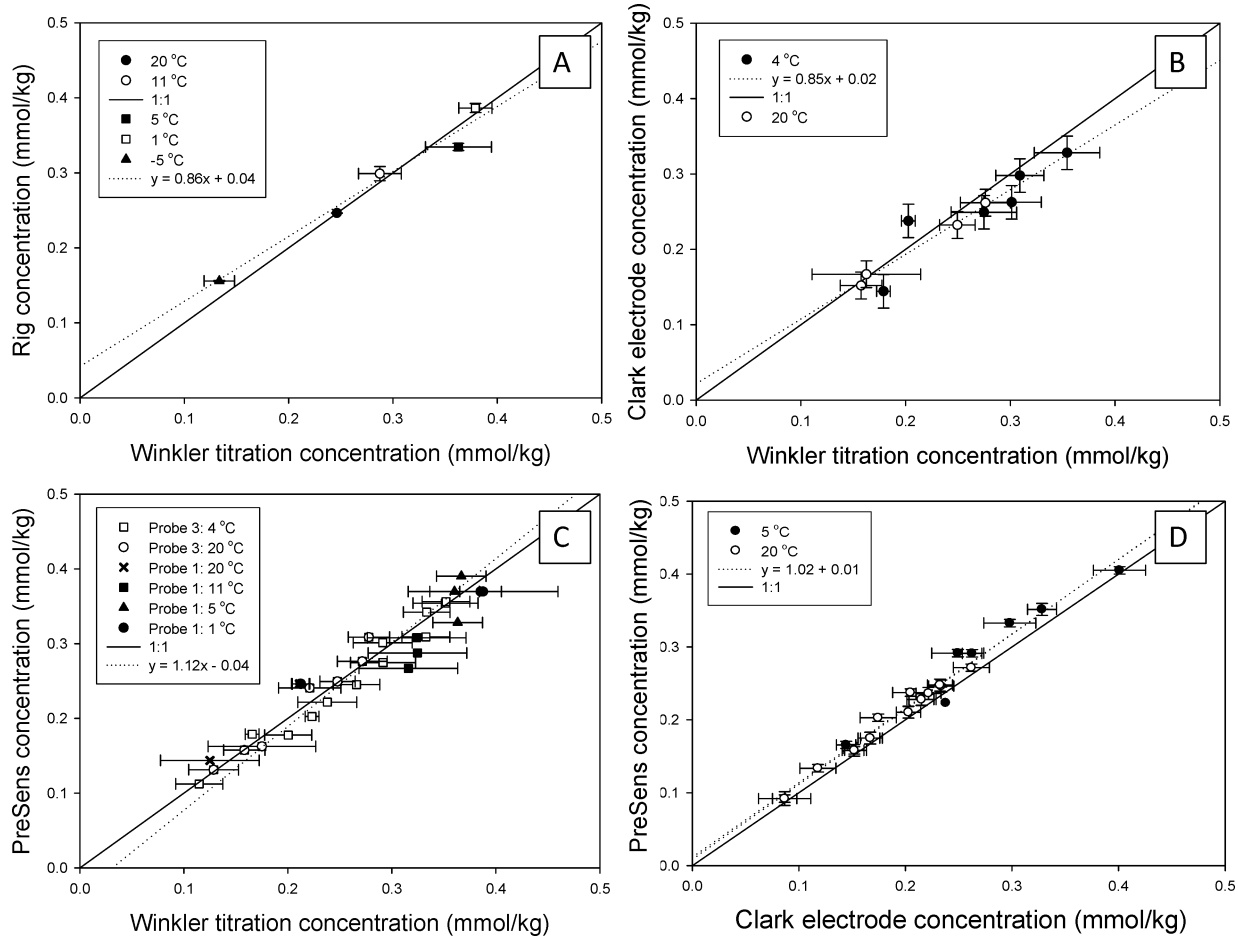

FIGURE 1. Comparison of the different methods available for measuring oxygen concentration. There is good agreement between the calibration rig and Winkler titration (a), between Winkler titration and the YSI Clark electrode (b) and the PreSens optode (c), and between the PreSens optode and Clark electrode (d). Precision is lowest for Winkler titration.

2 to 30 s, and an average was recorded on the logger every 1−15 min, with the timing dependent on the field test. Full details of field methods are given in the Supporting Information.

Results

Precision and Limit of Detection. The standard deviation of the noise in the phase shift signal recorded by the sensor film was measured over a 1 min interval with a frequency of 4 measurements per second. This was divided by the mean of the measurements to obtain the precision of the measurement. Precision varied with oxygen concentration, and there was little variation with temperature. The precision at 50 μmol/kg was ~0.6% (or ±0.3 μmol/kg) and at 300 μmol/kg was 0.4% (or ±1.25 μmol/kg). These values are comparable to that specified by the manufacturer (0.31 μmol/kg at 85 μmol/kg and 1.25 at 287 μmol/kg). The Limit of Detection (LoD) was defined as three times the standard deviation of the noise of the deoxygenated solution and was 0.9 μmol/kg at 1, 5, and 11 °C and 1.25 μmol/kg at 20 °C.

Response Time. All estimates of response time (t90) in solution were within the manufacturer's stated limit of <30 s. The t90 increased with decreasing temperature for both probe types tested (Supporting Information: Table 1, Figure II), reflecting enhanced permeability of the polymer support of the indicator dye at higher temperatures, due to higher solubility of molecular oxygen (*16, 29*). The t90 was faster in the gaseous phase for the dipping Probes (3 and 4) but slower for the needle-type Probe 2. This probably reflects the tendency for Probe 2 to retain solution in the housing for some time after the probe is moved into the air.

Drift Tests. The drift of Probe 2 was estimated over 90 h of measurements in deoxygenated water at 1.5 °C using a 1 s measurement frequency. The LED illumination was set to autoadjust, whereby the Oxyview software automatically alters the intensity of the LED to maintain stable signal amplitude. The sensor remained stable for the first 100k of the 320k measurements, with a mean measurement of 0.13 μmol/kg and a standard deviation of 0.1. Thereafter, there was measurable drift of approximately 1 μmol/kg in 300k measurements (Supporting Information: Figure III). The amplitude also began to decrease. The most likely explanation is that the sensor film suffered photobleaching (*22*). While this drift is small, in a field measurement situation it is possible to limit the intensity and duration of LED illumination and hence the duration of fluorophore excitation. This will reduce the degradation of the sensor film and the consequent drift rate. The drift of Probes 3 and 4 was monitored during the Swiss field deployment with constant LED illumination intensity (65%). Drift was estimated by inserting the probes into the calibration solutions (0 and 100% O_2 air-saturated). Both probes display drift rates (0.08−0.2%: Supporting Information: Table 1) that are well within PreSens quoted values (0.4% over 24 h, measuring every second).

Comparison with Other Methods. The DO concentrations measured by the calibration rig, Winkler titration, the PreSens optode (Probe 3), and the YSI Clark electrode are compared in Figure 1. Each comparison was conducted at a range of temperatures and repeated at least three times. The mean is displayed, and error bars are generated from the standard deviation of the repeated measurements. There was reasonable agreement between all three methods, with the slope

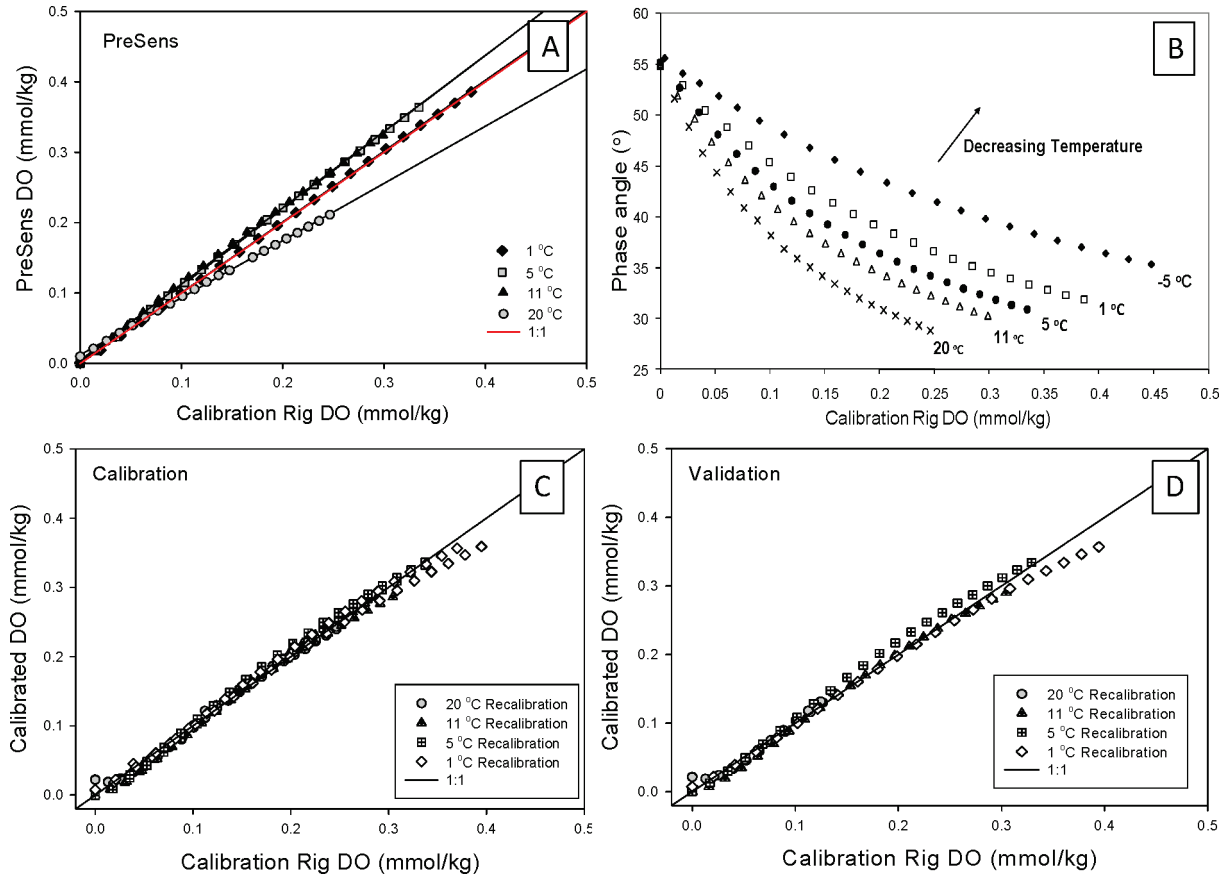

FIGURE 2. Probe 1 DO computed at a range of temperatures by a) the PreSens algorithm and calibration rig; (b) the PreSens raw phase shift and the calibration rig; and the new calibration algorithm and the calibration rig for (c) the calibration and (d) the validation data set.

of linear regression ranging from 0.85 ± 0.01 (YSI electrode vs Winkler titration, Figure 1b $r^2 = 0.91$, $n = 12$) to 1.12 ± 0.05 (PreSens optode (Probe 3) vs Winkler titration, Figure 1c, $r^2 = 0.88$, $n = 29$). Intercepts ranged from 0.04 to −0.04. The Clark electrode and the PreSens dipping probe gave very similar results, with slopes of near 1 and intercepts close to zero when compared with Winkler titration. There was divergence in the precision of the different methods, which was calculated by dividing the standard deviation of three repetitions of each measurement by the mean of these measurements. The precision of the YSI electrode ranged from 0.7−3%, with decreased precision at lower concentrations. The precision of the PreSens optode was 0.3% (see above). The precision of Winkler titrations performed on samples dispensed from the calibration rig was 6% and 11% on samples from the water bath. The precision of Winkler titration in a field laboratory is therefore significantly worse than both the PreSens optode and the YSI electrode.

Degradation Due to Freeze Thaw Cycles. Probe 3 performed well during freeze thaw cycling, retaining stable calibration readings throughout twenty freeze−thaw cycles. Probe 2 performed well for the first two cycles but failed by the end of the fifth cycle. Inspection under a microscope revealed that the probe tip had been damaged and that the sensor foil had become detached from the optical fiber (Supporting Information: Figure IV).

Temperature Dependence. Figure 2a shows the relationship between the absolute DO concentration provided by the calibration rig and that measured by the Microx sensors. The PreSens calibration performs well at some temperatures, particularly 1°C, but there is divergence from the 1:1 relationship at other temperatures. The divergence is more significant at higher oxygen concentrations, but deviations from the 1:1 line are not a linear function of temperature. For example, the Microx measurements are lower by up to 16% at 250 μmol/kg and 20 °C. By contrast, the relationship between the raw phase shift and oxygen concentration provided by the calibration rig varies systematically with temperature, such that increasing temperature produces a higher phase shift (Figure 2b). This suggests that the PreSens algorithm, which converts phase shift to oxygen concentration, does not completely compensate for temperature.

We subsequently sought to derive a temperature compensation procedure that provided a better fit to our data, using the Matlab 3D Surface Fitting Tool to fit a polynomial surface to our experimental data at 1, 5, 11, and 20 °C. The results of the improved calibration are shown in Figure 2c. We checked the calibration with a separate data set, shown in Figure 2d, which shows a more consistent fit to the data across the full range of temperatures than that produced by the PreSens software, particularly at intermediate to high oxygen concentrations. The residual sum of squares (RSS) across all temperatures was 0.082 for the PreSens algorithm and 0.014 for our new fit for the calibration data set and 0.180 and 0.172, respectively, for the independent validation data set. Testing the goodness of fit of both models showed that the recalibration performed marginally better than the PreSens algorithm, which was skewed (Figure V, Supporting Information). Statistical analysis of the fit at each temperature (Table 3, Supporting Information) shows that the recalibration performs more consistently across the range of temperatures tested, although the PreSens calibration is slightly better at 1°C. Since the temperature in glacial surface ecosystems may fluctuate by up to 8°C on a daily basis, the simpler algorithm may remove some of the uncertainties associated with the response of the PreSens algorithm to changing temperature.

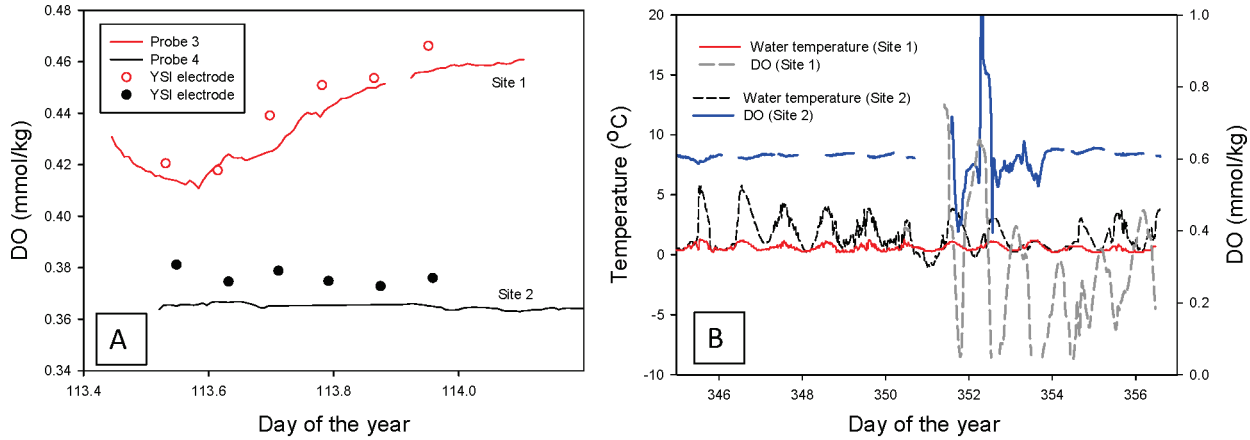

FIGURE 3. DO concentrations from field deployments in (a) Switzerland, in a snowmelt fed stream (Site 1, Probe 3) and a glacial meltwater stream adjacent to an anoxic groundwater seep (Site 2, Probe 4). Point measurements using the Clarke-type YSI electrode are also shown, which slightly overestimates DO. The discontinuous data set from the Antarctic deployment (b) reflects periodic temperature-induced sensor shut-down but is nevertheless the first high resolution record of DO from surface meltwater features on Antarctic glaciers.

Field Deployment. Probes 3 and 4 both survived field deployment at the Alpine and Antarctic sites. The sensors operated well with the dataloggers and were adequately powered with the solar charged 7Ah battery. However, at low temperatures (from −6.6 to 3.2 and −3.1 to +3.0 °C in Antarctica and the Alps, respectively), the optoelectronic units used for sensor interrogation did not retain power. They did not restart until the air temperature warmed sufficiently, or an external heat source was applied. For example, using chemically activated heating pads maintained adequate heating (see Supporting Information: Figures I and VI) for 3−8 h after application. The sensors recorded good data until the final two measurements before the transmitter shut down and returned to stable readings within two measurement points on restart.

Once processed to remove the effects of shutdown, the data provide a high resolution record of DO concentration in glacial meltwaters from the Arolla Valley (Figure 3). Site 2 was adjacent to a groundwater seep. The DO concentration was depleted throughout the monitoring period (mean DO air saturation of 88%), characteristic of groundwaters in subsurface environments where microbial respiration occurs (*30*). The record from Site 1 shows the influence of snowmelt, which introduces increasingly DO-saturated waters as the spring thaw proceeded. During the Antarctic test, colder temperatures result in more discontinuous data, but by the late season, warmer air temperatures and increased solar radiation enabled prolonged sensor operation. Waters remained undersaturated with oxygen for most of the season at Site 1, with the exception of a peak at Day 352 probably caused by freeze−thaw processes. At Site 2, the sensor recorded rapid variations in DO by Day 352, again as a result of rapid freeze−thaw fluctuations in a closed biogeochemical system. The scientific implications of these cycles are discussed in detail in ref *31*, but we believe that this is the first high resolution data set recording fluctuations in DO in a closed glacial aquatic environment.

Discussion

Results presented in this paper indicate that fiber optic sensors using luminescence lifetime indicators offer an excellent alternative to traditional methods for measuring DO in cryospheric environments. The most significant, but not insurmountable, problem experienced with the particular sensor used in this work (PreSens Fibox 3) during deployment is electronic failure at low temperatures. The cold temperature shut down can be managed with insulation and external heat sources, but further development in the electronics of these sensor packages is required to enable their use in long-term autonomous deployments to remote cryospheric environments (e.g., subglacial lakes). It is also important to select an appropriate sensor tip for the application because of the effects of freeze/thaw processes; here only sensors with a mechanically fixed sensor film survived freeze/thaw.

Fiber optic sensors are portable and require low power, response time is rapid, resolution and accuracy are high, and drift is minimal if sensor illumination is managed by either supporting software or a datalogger with pulsed trigger output. Precision is significantly better than Winkler titrations performed in the field environment, and the sensor has a number of advantages over a Clark-type electrode. Most significantly, Clark electrodes require constant stirring, either manually or through a constant water flow rate. The flow dependence can be up to 25% of the recorded concentration (*32*). The membrane of a Clark electrode is also susceptible to decay, with a manufacturer specified lifetime of 2 to 8 weeks.

A number of authors have used fiber optic sensors successfully to measure biogeochemical variables in marine and freshwater environments (*15, 21, 22*), but there have been very few applications in the Cryosphere to date. Mock et al. (*23*) describe the application of micro-optodes, similar to the exposed silica fiber Probe 1 described here, in a model sea ice environment. The optodes were frozen into a sea ice mesocosm, with the luminescence lifetime interrogator remaining at standard room temperatures. No cold temperature shut-down problems occurred because the interrogator was housed in a warm environment. The model sea ice experiment did not incorporate freeze−thaw cycles but rather a single freezing event. Our data show that microprobes (Probes 1 and 2) are unlikely to survive multiple freeze−thaw events. This suggests that micro-optodes may not be ideal for long-term deployment in sea ice or any environment where freezing and thawing conditions prevail. Here, dipping probes (e.g., Probes 3 and 4) may be more suitable where multiple freeze−thaw cycles are expected.

In addition, the PreSens algorithm, which computes DO concentrations from the recorded phase shift, performed well at 1 °C but was not consistent across the whole temperature range. We used a simpler 3D polynomial fit that produced DO concentrations which were consistent with those delivered by the calibration rig at the full range of temperatures used. Depending on the accuracy required and the measurement temperature range, the raw phase shift

could be postprocessed using the simpler 3D algorithm reported in this manuscript.

High resolution monitoring of glacial biogeochemical processes has great potential to increase our understanding of how life operates at the limits of survival (*31*). We believe that the use of fiber optic sensors in long-term monitoring provides the glacial biogeochemical community with a new opportunity to expand understanding of how glacial ecosystems operate throughout a full annual cycle. This study has assessed the performance of fiber optic probes in glacial environments and has demonstrated their compatibility with this environment, if some obstacles can be overcome (e.g., low temperature tolerance of electronics, freeze−thaw survival). Further iterations of the tested technologies are required to enable autonomous deployments to more remote glacial habitats, (e.g., design modifications to enable low temperature operation, and volume reduction of the sensor/logging package). This is particularly true for the exploration of Antarctic subglacial lakes and other subice sheet aquatic systems (*1*) and ultimately in the exploration of water bodies on other planets (*33*).

Acknowledgments

This work was supported by EPSRC grant EP/D057620/1 and NSF grant ANT-0423595. Fieldwork was conducted with the McMurdo Dry Valleys LTER site team whose support is gratefully acknowledged, with logistics provided by Raytheon Polar Services and PHI Helicopters. The manuscript was greatly improved by the comments of three anonymous reviewers.

Supporting Information Available

Text, Tables 1-3, and Figures I-VI. This material is available free of charge via the Internet at http://pubs.acs.org.

Literature Cited

(1) Siegert, M. J.; Carter, S.; Tabacco, I.; Popov, S.; Blankenship, D. D. A revised inventory of Antarctic subglacial lakes. *Antarct. Sci.* **2005**, *17* (3):), 453–460.

(2) Sharp, M.; Parkes, J.; Cragg, B.; Fairchild, I. J.; Lamb, H.; Tranter, M. Widespread bacterial populations at glacier beds and their relationship to rock weathering and carbon cycling. *Geology* **1999**, *27* (2), 107–110.

(3) Wadham, J. L.; Tranter, M.; Tulaczyk, S.; Sharp, M. Subglacial methanogenesis: A potential climatic amplifier. *Global Biogeochem. Cycles* **2008**, *22* (2), 16.

(4) Tranter, M.; Sharp, M. J.; Lamb, H. R.; Brown, G. H.; Hubbard, B. P.; Willis, I. C. Geochemical weathering at the bed of Haut Glacier d'Arolla, Switzerland - a new model. *Hydrol. Processes* **2002**, *16* (5), 959–993.

(5) Priscu, J. C.; Wolf, C. F.; Takacs, C. D.; Fritsen, C. H.; Laybourn-Parry, J.; Roberts, E. C.; Sattler, B.; Lyons, W. B. Carbon transformations in a perennially ice-covered Antarctic lake. *Bioscience* **1999**, *49* (12), 997–1008.

(6) Hodson, A.; Anesio, A. M.; Tranter, M.; Fountain, A.; Osborn, M.; Priscu, J.; Laybourn-Parry, J.; Sattler, B. Glacial ecosystems. *Ecol. Monogr.* **2008**, *78* (1), 41–67.

(7) Anesio, A. M.; Hodson, A. J.; Fritz, A.; Psenner, R.; Sattler, B. High microbial activity on glaciers: importance to the global carbon cycle. *Global Change Biol.* **2009**, *15* (4), 955–960.

(8) Carpenter, J. H. The Chesapeake Bay Institute technique for the Winkler Dissolved Oxygen method. *Limnol. Oceanogr.* **1965**, *10* (1):), 141–143.

(9) Bryan, J. R.; Riley, J. P.; Williams, P. J. L. Winkler Procedure for making precise measurements of Oxygen concentration for productivity and related studies. *J. Exp. Mar. Biol. Ecol.* **1976**, *21* (3):), 191–197.

(10) Clark, L. C.; Wolf, C. F.; Granger, D.; Taylor, Z. Continuous recording of blood oxygen tensions by polarography. *J. Appl. Physiol.* **1953**, *6* (3):), 189–193.

(11) Bagshaw, E. A.; Tranter, M.; Fountain, A. G.; Welch, K. A.; Basagic, H.; Lyons, W. B. Biogeochemical evolution of cryoconite holes on Canada Glacier, Taylor Valley, Antarctica. *J. Geophys. Res., [Biogeosci.]* **2007**, *112* (G4), 8.

(12) Tranter, M.; Fountain, A. G.; Fritsen, C. H.; Lyons, W. B.; Priscu, J. C.; Statham, P. J.; Welch, K. A. Extreme hydrochemical conditions in natural microcosms entombed within Antarctic ice. *Hydrol. Processes* **2004**, *18* (2), 379–387.

(13) Ebnet, A. F.; Fountain, A. G.; Nylen, T. H.; McKnight, D. M.; Jaros, C. L. A temperature-index model of stream flow at below-freezing temperatures in Taylor Valley, Antarctica. *Ann. Glaciol.* **2005**, *40,* 76–82.

(14) Lippitsch, M. E.; Pusterhofer, J.; Leiner, M. J. P.; Wolfbeis, O. S. Fibre-optic oxygen sensor with the fluorescence decay time as the information carrier. *Anal. Chim. Acta* **1988**, *205* (1−2), 1–6.

(15) Klimant, I.; Meyer, V.; Kuhl, M. Fibreoptic Oxygen Microsensors: A new tool in aquatic biology. *Limnol. Oceanogr.* **1995**, *40* (6), 1159–1165.

(16) Wolfbeis, O. S. Fiber-optic chemical sensors and biosensors. *Anal. Chem.* **2008**, *80* (12), 4269–4283.

(17) Rogers, K. R.; Poziomek, E. J. Fiber optic sensors for environmental monitoring. *Chemosphere* **1996**, *33* (6), 1151–1174.

(18) Okeeffe, G.; Maccraith, B. D.; McEvoy, A. K.; McDonagh, C. M.; McGilp, J. F. Development of a LED-based phase fluorometric oxygen sensor using evanescent-wave excitation of a sol-gel immobilised dye. *Sens. Actuators, B* **1995**, *29* (1−3), 226–230.

(19) Draxler, S.; Lippitsch, M. E.; Klimant, I.; Kraus, H.; Wolfbeis, O. S. Effects of polymer matrices on the time-resolved luminescence of a Ruthenium complex quenched by oxygen. *J. Phys. Chem.* **1995**, *99* (10), 3162–3167.

(20) Demas, J. N.; DeGraff, B. A.; Coleman, P. B. Oxygen sensors based on luminescence quenching. *Anal. Chem.* **1999**, *71* (23), 793A–800A.

(21) Tengberg, A.; Hovdenes, J.; Andersson, H. J.; Brocandel, O.; Diaz, R.; Hebert, D.; Arnerich, T.; Huber, C.; Kortzinger, A.; Khripounoff, A.; Rey, F.; Ronning, C.; Schimanski, J.; Sommer, S.; Stangelmayer, A. Evaluation of a lifetime-based optode to measure oxygen in aquatic systems. *Limnol. Oceanogr.: Methods* **2006**, *4*, 7–17.

(22) Warkentin, M.; Freese, H. M.; Karsten, U.; Schumann, R. New and fast method to quantify respiration rates of bacterial and plankton communities in freshwater ecosystems by using optical oxygen sensor spots. *Appl. Environ. Microbiol.* **2007**, *73* (21), 6722–6729.

(23) Mock, T.; Dieckmann, G. S.; Haas, C.; Krell, A.; Tison, J. L.; Belem, A. L.; Papadimitriou, S.; Thomas, D. N. Micro-optodes in sea ice: a new approach to investigate oxygen dynamics during sea ice formation. *Aquat. Microb. Ecol.* **2002**, *29* (3), 297–306.

(24) Kilmant, I.; Ruckruh, F.; Liebech, G.; Stangelmayer, A.; Wolfbeis, O. S. Fast response oxygen micro-optodes based on novel soluble ormosil glasses. *Microchim. Acta* **1999**, *131*, 35–46.

(25) Langmuir, D. *Aqueous Environmental Geochemistry*; Prentice Hall: NJ, 1997.

(26) PreSens. *Instruction Manual Fibox 3*; Regensburg, 2006.

(27) Sosna, M.; Denuault, G.; Pascal, R. W.; Prien, R. D.; Mowlem, M. Field assessment of a new membrane-free microelectrode dissolved oxygen sensor for water column profiling. *Limnol. Oceanogr.: Methods* **2008**, *6*, 180–189.

(28) Hydes, D. J.; Hartman, M. C.; Kaiser, J.; Campbell, J. M. Measurement of dissolved oxygen using optodes in a FerryBox system. *Estuarine, Coastal Shelf Sci.* **2009**, *83*, 485–490.

(29) Kocincova, A. S.; Borisov, S. M.; Krause, C.; Wolfbeis, O. S. Fiber-optic microsensors for simultaneous sensing of oxygen and pH, and of oxygen and temperature. *Anal. Chem.* **2007**, *79* (22), 8486–8493.

(30) Baker, M. A.; Valett, H. M.; Dahm, C. N. Organic carbon supply and metabolism in a shallow groundwater ecosystem. *Ecology* **2000**, *81* (11), 3133–3148.

(31) Bagshaw, E. A., Wadham, J. L., Tranter, M., Fountain, A. G., Mowlem, M. High resolution monitoring reveals dissolved oxygen dynamics in an Antarctic cryoconite hole. *Hydrol. Processes*, Submitted.

(32) YSIEnvironmental. *YSI 550A operations manual*; Yellow Springs, OH, 2006.

(33) Bortman, H. *Probing Antarctica's Lake Bonney*, in *Astrobiology Magazine*. NASA: 2009.

(34) Standard Methods for the examination of water and wastewater. Standard Methods, Ed. A.P.H. Association, Association, A.W.W., and Federation, W.E., Eaton, A. D., Clesceri, L. S., Greenberg, A. E. Eds.; American Public Health Association: Washington, DC, 1995.

(35) Fountain, A. G.; Nylen, T.; Tranter, M.; Bagshaw, E. A. Temporal variation of cryoconite holes on Canada Glacier, McMurdo Dry Valleys, Antarctica. *J. Geophys. Res.* **2008**, *112*, (G01S92).

ES102571J